

---

# High-angular diffusion MRI in reward-based psychiatric disorders

# 2

Wenwen Yu, Qiming Lv, Chencheng Zhang,  
Zhuangming Shen, Bomin Sun and Zheng Wang

---

## Abstract

The structural mapping of the complex brain networks under healthy and diseased states is of great importance to understand the working mechanism of the brain function. Diffusion weighted magnetic resonance imaging and its derivative methods are currently the only way to measure macroscopic axonal organization in nervous system tissues, in vivo and non-invasively. Nevertheless, it has revealed tremendous unprecedented details about the brain architecture and inspired unlimited expectation on its future development. In this chapter, we first explain the basic principles of diffusion tensor imaging (DTI), and then discuss the strategies for resolving multiple fibers within one voxel, in particular on the diffusion spectrum imaging (DSI) method. We further introduce the pipeline of data analysis including quantification of whole brain white matter and visualization of specific microstructural tracts, and conclude with their recent applications in psychiatric disorders.

---

## Keywords

Magnetic resonance imaging · Diffusion tensor imaging · Diffusion spectrum imaging · Tractography · Fiber crossing · Neuroanatomy

---

## 2.1 Introduction

Diffusion-weighted magnetic resonance imaging (DW-MRI) is an emerging magnetic resonance imaging (MRI) method ever since the mid-1980s [7, 37, 62], which allows the detecting of the diffusion process of water molecules in biological tissues, in vivo and non-invasively. By calculating the biophysical trajectory of water diffusion to infer the architecture of the white matter, diffusion tensor imaging (DTI) has become one of the most valuable MRI techniques

---

W. Yu · Q. Lv · Z. Shen · Z. Wang (✉)  
Institute of Neuroscience, Shanghai Institutes for  
Biological Sciences, Chinese Academy of Sciences,  
320 Yueyang Road, Shanghai 200031, China  
e-mail: zheng.wang@ion.ac.cn

C. Zhang · B. Sun  
Department of Functional Neurosurgery, Ruijin  
Hospital, School of Medicine, Shanghai Jiaotong  
University, Shanghai 200025, China

of pursuing the working mechanism of brain architecture [26, 33, 43, 56]. Furthermore, assessment of the microstructural integrity of the axonal fibers using a variety of diffusion indices has absorbed an increasing attention in the study of neurological diseases or psychiatric disorders [4, 5, 13, 25, 32, 45].

This chapter starts from some theoretical background of diffusion derived MRI methods including the widely-accepted DTI and newly-developed diffusion spectrum imaging (DSI), and introduces some popular algorithms available for in vivo constructing tractography, as illustrated with some classic white matter (WM) fiber tracts. Finally it concludes with short summary of their current clinical applications in a wide range of psychiatric disorders. It is reasonably expected that such kind of discussion could catalyze the technological development in the light of meeting the clinical needs, and vice versa foster more potential applications for various categories of diagnostic purposes.

## 2.2 How DTI Works

The human body is made up of over 70 % water, in which the incessant random motion of water molecules is influenced by distinct kinds of restricted factors such as cell membranes, cytoskeleton, and macromolecules [26]. Because diffusional processes are influenced by the geometrical structure of the biological environment, diffusion MRI, has been successfully demonstrated to characterize diffusion displacement of water molecules and reveal the underlying microstructure in vivo [14, 16, 53, 66]. In spite of its recent introduction to brain imaging, tensor-based diffusion MRI has inspired a rising wave of biomedical applications of quantifying the diffusional characteristics of a wide range of specimens. In particular, for brain diseases diagnostics, DTI has been successfully used to demonstrate subtle abnormalities in a variety of neurological diseases (including stroke, multiple sclerosis, dyslexia, schizophrenia, and Alzheimer's disease) and is currently becoming an

indispensable part of many routine clinical protocols [4, 13, 25, 32, 34, 40, 48, 50, 63]. The diffusion pattern of water molecules can be simplified by the diffusion tensor model, which makes it feasible to show the gross fiber orientation and provide quantitative descriptions such as fractional anisotropy (FA) and diffusivity [54]. As such, more unique insights into tissue microstructure can be gained through the use of these indices: diffusion anisotropy as a useful index of white matter integrity and estimated orientation of the principal direction of axon fibers to enable tractography [21, 23]. These unprecedented information obtained from DTI studies are hence increasingly invaluable to both clinical physicians and scientific researchers.

Here we present a brief overview of the basic principles of DTI method and the readers can consult to the literature for more in-depth technical details [10, 26]. In essence, diffusion MRI measures the dephasing of spins of protons in the presence of a spatially-varying magnetic field ('gradient'), which changes their Larmor frequency [37, 59, 62]. The intuitive mechanism here is the phase change resulting from components of incoherent displacement of spins along the axis of the applied field gradient. For stationary (non-diffusing) molecules, the phases induced by both gradient pulses will completely cancel so as to lead the maximally coherent magnetization and there will be no signal loss from diffusion [27]. In the case of coherent flow in the direction of the applied gradient, the bulk motion will cause the signal phase to change by different amounts regarding to each pulse so that there will be a net phase difference. Therefore, in the presence of diffusion gradients, water molecules will accumulate different phases, and the phase dispersion from diffusion will cause signal attenuation,  $S$ .

$$S = S_0 e^{-bD} \quad (2.1)$$

where  $S$  is the DW signal,  $S_0$  is the signal without any DW gradients (but otherwise identical imaging parameters),  $D$  is the apparent diffusion coefficient, and  $b$  is so-called "b-factor". MRI signals are proportional to the sum of

magnetization components from all water molecules in a voxel, which is closely associated with the area of the diffusion gradient pulses defined by the amplitude of the magnetic field gradient pulses,  $G$ , and the temporal duration,  $\delta$ , and the temporal spacing between the pulses,  $\Delta$ . The effects of all these parameters are indeed ascribed to a coarse term “b-factor” as below:

$$b = \gamma^2 G^2 \delta^2 (\Delta - \delta/3) \quad (2.2)$$

where  $\gamma$  is the gyromagnetic ratio.

By applying the appropriate magnetic field gradients, MR imaging may be sensitized to the random, thermally driven motion (diffusion) of water molecules in the direction of the field gradient. Diffusion is anisotropic (directionally dependent) in WM fiber tracts, as axonal membranes and myelin sheaths present barriers to the motion of water molecules in directions not parallel to their own orientation. The direction of maximum diffusivity has been shown to coincide with the orientation of WM fiber tracts [44].

In short, the fundamental concept behind DTI is that water molecules diffuse differently in the tissues heavily depending on its type, integrity, architecture, and presence of barriers, generating information about its orientation and quantitative anisotropy embodied by the diffusion tensors [9, 14, 44]. DTI may be used to map and characterize the three-dimensional diffusion pattern as a function of spatial location, which can further be taken advantage of estimating the connectivity properties of the whole brain WM networks, using the diffusion anisotropy and the principal diffusion directions [23].

Undoubtedly, DTI holds a unique and unparalleled sensitivity to water movements of painting the blueprint of brain architecture [26, 33, 43, 56], as uses existing MRI technology without the necessity of investing new equipment, contrast agents, or even radiochemical tracers. However, there remain many technical issues with regard to the performance of the tool, practical considerations of working on biological specimens, and the interpretation of DTI tractography images. For instance, within each voxel of diffusion-encoded images, it can only resolve

the single (the most dominant) fiber direction and cannot differentiate the kissing/crossing/branching fibers in the complex cerebral regions [1, 71]. Consequently it estimates the fiber orientation to be the mean of the underlying fiber directions, even though the mean direction will not be representative of the true fiber directions [3]. Nevertheless, it is not capable of determining with accuracy the origin and destination of fibers, which requires further comprehensive evidence to corroborate, even in combination with employing other advanced technologies [5, 58].

## 2.3 Diffusion Spectrum MRI (DSI)

Recent technological development of MRI methods has been devoted to solving the aforementioned issues, so as to better characterize the complicated fiber patterns and discern fiber orientations. As matter of a fact, either model-based or model-free methods have been acknowledged that have the capacity to resolve heterogeneity of fiber orientations in each resolved volume of tissue (voxel) [65, 68], and provide detailed views into the precise organization of cerebral white matter tracts [69]. Here we will focus on the model-free derivations of diffusion MRI technique.

Model-free methods, also called q-space imaging methods [11, 16, 59], measure the microscopic diffusion function directly without any assumptions on the form of the underlying diffusion function, even though they still have to count on the Fourier transform relation between the diffusion MR signals and the underlying diffusion displacement [31]. Firstly the probability density function (PDF) or orientation distribution function (ODF) of the diffusion displacement in the three biophysical dimension are obtained. One can then calculate a common quantitative scalar measure, generalized fractional anisotropy (GFA) in DSI, physiologically equivalent to FA [19], so as to implicate the microstructure property. Worthy to mention, FA, an index derived from the diffusion tensor that reflects the degree of directional coherence, myelination, and

diameter of axonal fibers has been widely used to examine the integrity of white matter tracts in DTI [4, 26]. Simply put, higher FA or GFA values imply higher coherence of fiber directions, more myelination or larger axonal diameters in the white matter at the microstructural level.

More frequently the connections of each ODF will be explored to infer the underlying linking patterns of the fibers [22]. Here in after, we briefly discuss two commonly used q-space (diffusion-encoding space) reconstruction methods to estimate the ODF from the acquired diffusion MR signals, with particular emphasis on the DSI method.

**Q-ball imaging (QBI):** Tuch and his co-workers introduced q-ball imaging (QBI) [64], which usually used the Funk–Radon transform (also known as the spherical Radon transform) to reconstruct ODF at the cost of large pulsed field gradient and time-intensive sampling. It is also feasible to resolve intravoxel fiber crossing through using a high angular resolution diffusion imaging (HARDI) scheme, which samples data on a shell in the diffusion encoding space. The Funk–Radon transform relation forms the core basis of the QBI reconstruction method to avoid any assumptions on the diffusion process like Gaussianity or multi-Gaussianity and to achieve better accuracy and efficiency [17].

**Diffusion spectrum imaging (DSI):** Wedeen and his colleagues proposed to acquire the diffusion MR signals by using the grid sampling scheme, and then applied the Fourier transform on the q-space data to estimate the underlying diffusion displacement pattern for further calculation of the ODF [15, 21, 31, 61, 65, 68–70, 72]. The sampling scheme of DSI produces a cluster of grid points distributed on a sphere in the q-space. Each grid point corresponds to a specific value of diffusion sensitivity (b-value) and direction, and the b-value increases incrementally from 0 to a maximal b-value (b-max). When all the diffusion-encoding samples in the q-space have been collected, the Fourier transform (FT) is performed to obtain the PDF as the diffusion-encoding samples  $S(q)$  and their corresponding PDFs constitute a Fourier pair [10]. In sum, DSI measures the ODF by acquiring hundreds of

diffusion-weighted images (DWI) with different diffusion-encoding gradients, each with different strength and direction [5, 21]. In this manner, it is possible to infer the number of fiber-compartments and their relative amplitude as well as spatial orientations by reconstructing the ODF local maxima. It enables DSI to resolve kissing or crossing or bending fiber orientations at single voxel-based level, as shown in Fig. 2.1.

Bear in mind, though, some precautions should be carefully exercised when implementing these two q-space imaging methods to derive diffusion ODF. One caveat of the QBI method is that the acquired diffusion MR signal is in fact contributed by the diffusion displacements in all directions, not just the displacements perpendicular to the diffusion gradient vector. Consequently the q-ball ODF can only be deemed as good approximation since it doesn't consider all diffusion displacements in the three-dimensional space [62]. On the other hand, DSI is able to characterize the diffusion probability density function by applying the Fourier transform to the MR signals in the q-space; however, it still relies on numerical estimation to calculate the ODF. The mathematical estimation often encounters the truncation artifacts in the Fourier transform, as entails additional treatment like a Hanning filter smoothing on the PDF [22, 31].

**Generalized-sampling imaging (GQI):** Recently the spin distribution function (SDF) has been defined to quantitatively describe a distribution of the spins undergoing diffusion on the voxel basis, which is unlike the diffusion ODF representing a probability distribution of the diffusion displacement [72]. This relation leads to an imaging method named generalized q-sampling imaging (GQI) which is readily applicable to a wide range of q-space datasets including those acquired by the shell or grid sampling schemes. Taking a closer look at the reconstruction equations of GQI and DSI, they share the same theoretical basis. Hence GQI and DSI reconstruction could result in similar diffusion patterns. Note that the reconstruction process of GQI does not require deconvolution procedures and the SDF values can be compared across voxels [72].

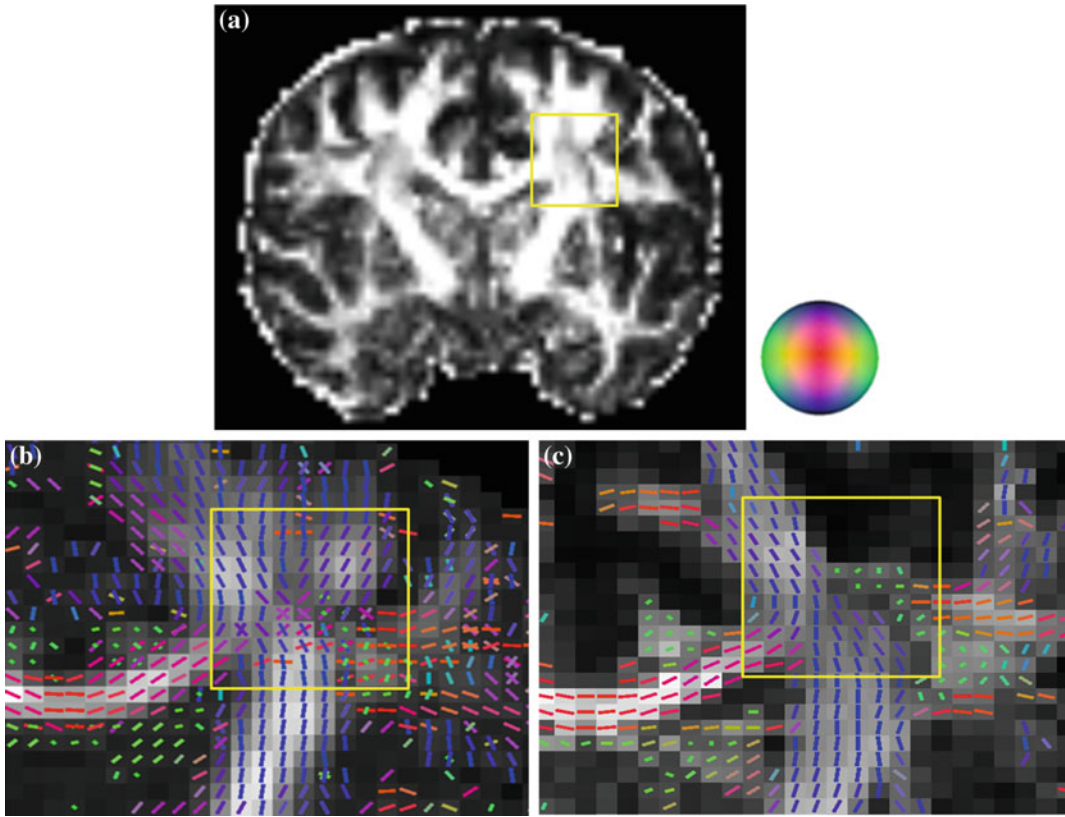


**Fig. 2.1** Comparison on the fiber orientations of the centrum semiovale resolved by DTI and DSI on the same subject. **b** Using DSI, fibers coursing towards the corpus callosum (*red*) intersect with vertically oriented corona radiata fibers (*blue*) and rostro-caudally oriented long association fibers (*green*). In contrast to using DTI (**c**), only one fiber orientation is seen within one voxel. **a** DTI-

derived FA map. The area within *yellow boxes* of each image **a**, **b**, **c** is the centrum semiovale. The directions of the ODF or SDF are pseudo-colored: *red* in the left-right direction, *green* in the anterior-posterior direction, and *blue* in the axial superior-inferior direction, illustrated by the color ball. The *gray* background represents the calculated values of GFA (**b**) and FA (**c**), respectively

## 2.4 Diffusion MR Tractography

Tractography has been developed to improve the depiction of data from diffusion imaging of the brain and aid the image interpretation [8, 67]. The primary purpose of tractography is to clarify the orientational architecture of nerve fibers by integrating pathways of maximum diffusion coherence. The computational algorithms normally track the diffusion maximum from voxel to voxel in such a way of simulating the fibers growing across the brain. The fibers offered by tractography are often accepted to represent individual axons or nerve fibers, but they are more

accurately viewed as lines of dominant diffusion that follow or parallel the local diffusion maxima [43]. This distinction is vital because, given with certain imaging resolution and signal-to-noise level, lines of maximum diffusion coherence may differ from the axonal architecture in some brains [42]. For example, DTI provides a Gaussian approximation of the actual displacement distribution, and since the representation of that distribution is restricted to variations of an ellipsoid, this method creates various biases in the resulting tractography [27]. Also the tractography results depend on the tracking algorithm used. Deterministic fiber tracking from DTI uses the principal direction of diffusion to integrate trajectories



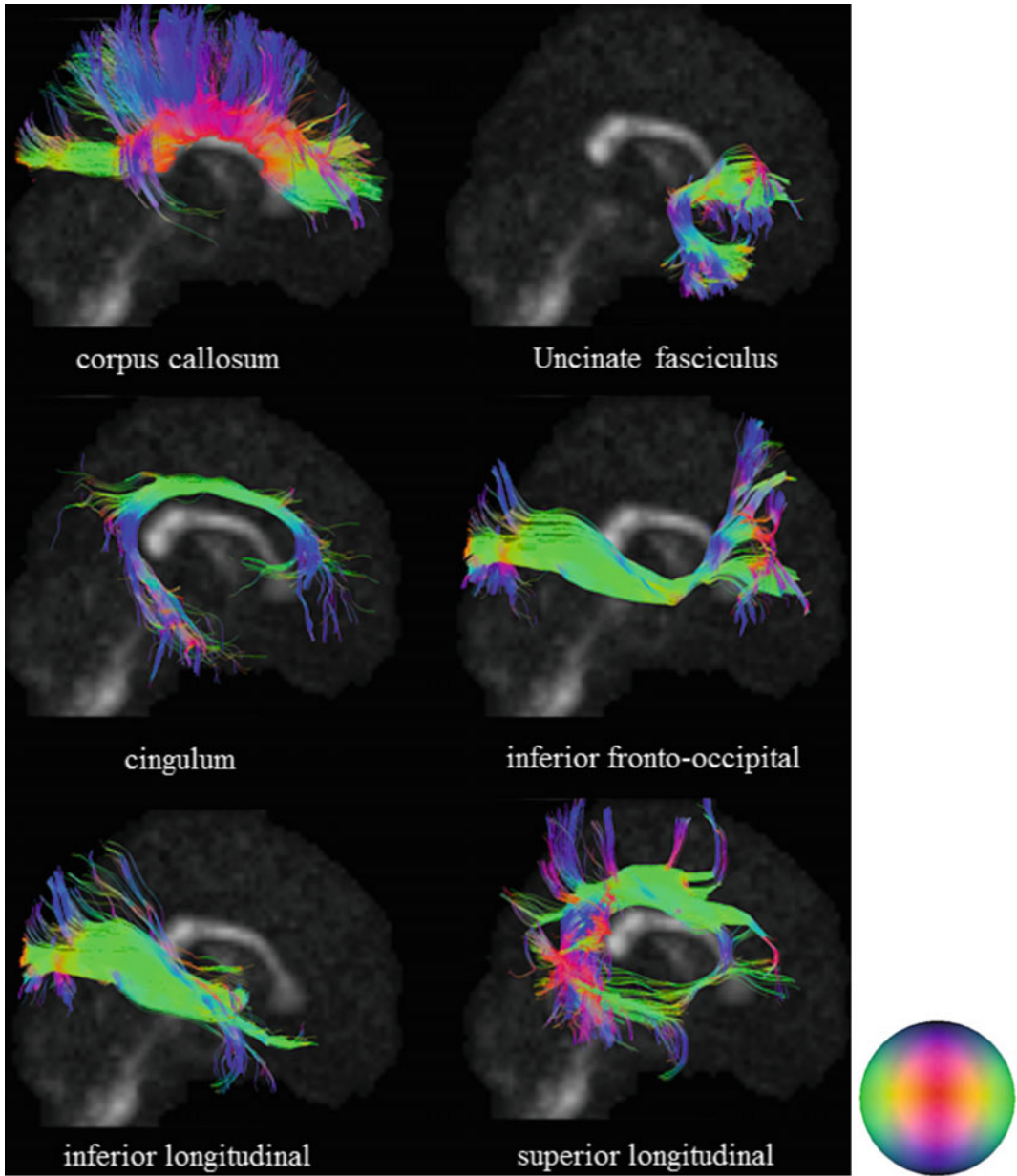


**Fig. 2.2** Six classic white matter tracts obtained with DSI tractography (overlay on sagittal views of GFA maps)

over the image but ignores the fact that fiber orientation is often undetermined in the diffusion tensor imaging data [42].

The fact is that the connectivity maps obtained with tractography vary according to the diffusion imaging modality used to obtain the diffusion datasets. Hagmann and colleagues investigated statistical fiber tracking methods based on

consideration of the tensor as a probability distribution of fiber orientation [23]. The application of fiber tractography to data such as those obtained with DSI or QBI results in the depiction of a large set of fiber tracts with a more complex geometry. Such greater complexity obtained with this method is due to the consideration of numerous intersections between fibers that can

be resolved or differentiated. In such sense, DSI tractography overcomes some above biases and allows more realistic mapping of connectivity [21, 31, 69, 70]. Figure 2.2 presents typical examples of six major white matter tracts reconstructed by DSI.

Nonetheless, tractography provides more interesting and valuable information for depicting the human neuroanatomy in vivo.

## 2.5 Procedure of Data Analysis

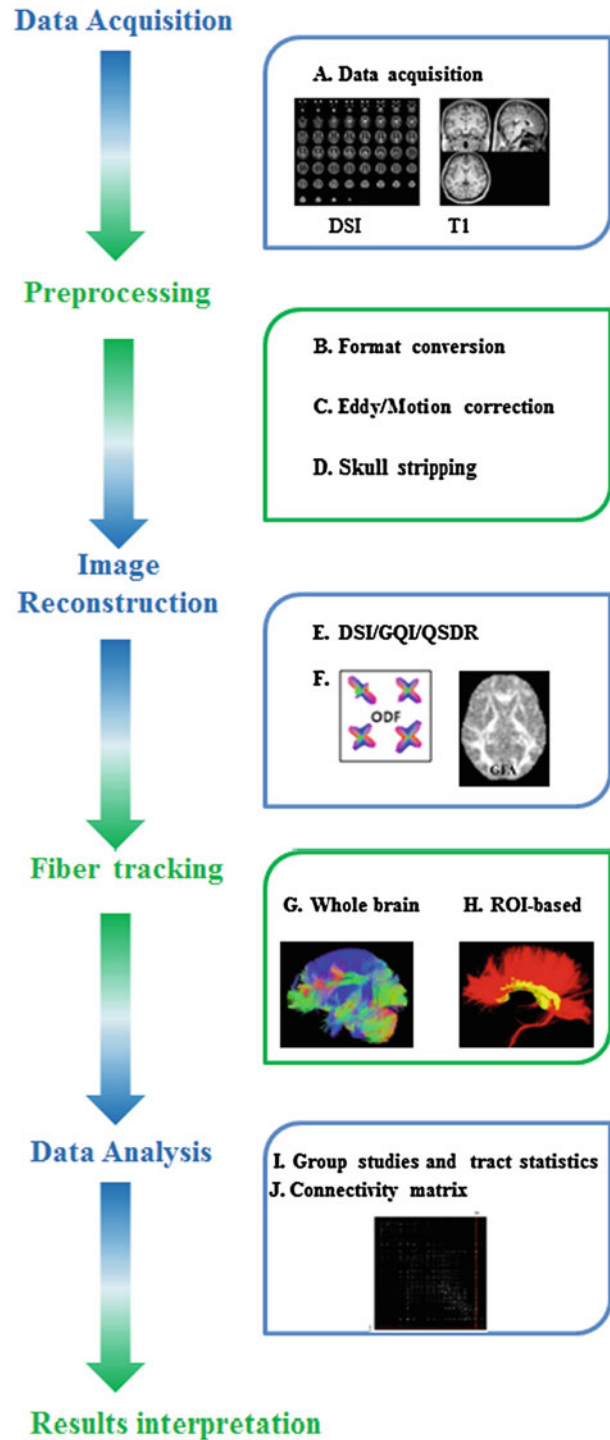
Here we used the DSI image dataset collected by Functional Brain Imaging Platform (FBIP) at Institute of Neuroscience, Chinese Academy of Sciences, Shanghai, to demonstrate the procedure widely-used in the analysis of the diffusion MRI data. It will lend the support to those who are interested in applying these neuroimaging techniques to solve those clinically-driven problems during diagnostics and therapy of psychiatric disorders. A schematic workflow diagram of diffusion MRI processing is illustrated in Fig. 2.3.

The detailed imaging protocol will be described in other places and summarized shortly here. T1-weighted structural MRI images were acquired on a 3T MR imaging system (Magnetom Trio; Siemens, Erlangen, Germany) using a 12-channel phased array head coil (TR = 2,300 ms, TE = 3 ms, TI = 1,000 ms, flip angle =  $9^\circ$ , FOV =  $256 \times 256$  mm<sup>2</sup>, voxel size =  $1.0 \times 1.0 \times 1.0$  mm<sup>3</sup>, 176 slices, no slice gap). Earplugs were used, and movement was minimized by stabilizing the head with cushions. Diffusion spectrum imaging was acquired using a twice-refocused spin-echo EPI pulse sequence [55]. The diffusion-encoding scheme used in this study followed the framework of DSI in which diffusion-weighted images were acquired with diffusion gradients of different b values corresponding to the grid points filled within a sphere in the 3D diffusion-encoding space (q-space) [68]. TR = 9,500 ms,

TE = 152 ms, flip angle =  $90^\circ$ , FOV =  $80 \times 80$  mm<sup>2</sup>, voxel size =  $2.4 \times 2.4 \times 2.4$  mm<sup>3</sup>, b-max = 7,000 s/mm<sup>2</sup>. To reduce the scan time, we only recorded half-sphere DSI data [20, 21]. Specifically, the DSI data were acquired with 128 diffusion-encoding directions corresponding to grid points filled in the half sphere of the q-space. Acquisition time for the half-scheme acquisition was 21 min. To correct for image distortion resulting from magnetic susceptibility, field maps were acquired using a GRE sequence with two TEs (acquisition time, 91 s, TR/TE = 500/3.38 and 5.84 ms). The matrix size and FOV of the field maps were the same as those used in the DSI dataset.

The half-sphere data were extrapolated to the other half of the sphere based on the symmetry property of the data in the q-space, and the eight corners of the cube that were unsampled were zero-filled. The susceptibility-induced distortion on each DSI image was first corrected using the acquired field maps [24], and then subjected to the motion correction and eddy current compensation using the software based on FSL (<http://www.fmrib.ox.ac.uk/fsl>). The following DSI data reconstruction was conducted through using the generalized q-sampling imaging approach available in the software of DSI Studio (<http://dsi-studio.labsolver.org>) [15]. The ODFs were reconstructed to 162 discrete sampling directions (corresponding to the vertices of a 4-fold regularly tessellated icosahedron projected onto the sphere). The diffusion deconvolution was then applied to the diffusion ODFs generated from GQI to increase the angular resolution of the resolved fiber. Having obtained the ODF, the GFA (similar to FA) was derived to quantify the directionality of the diffusion on a scale from zero (when the diffusion was totally random) to one (when the diffusion was along one direction only). The formula of deriving the value of GFA is defined as the ratio of the standard deviation of ODF and its root mean square [64]. Like FA, GFA has been used to infer microstructure integrity of the white matter fiber tracts.

**Fig. 2.3** A schematic diagram of typical DSI data-processing workflow. Step 1: Data acquisition (A). Step 2: Preprocessing includes the conversion of original dataformat (B), eddy and motion correction (C), and skull stripping (D). Step 3: Image reconstruction. Some commonly-used reconstruction approaches are listed here like DSI, GQI or QSDR (E). The ODFs or GFA are calculated for further analysis (F). Step 4: Fiber tracking. Either the whole-brain (G) or ROI-based fiber tracking (H) can be chosen for distinct research objectives. Step 5: Data analysis. Statistical comparison of fiber tracts can be conducted at group-level (I and J) and the network-level analysis can be used to extract more features from the structural connectivity matrix





In addition to subject-specific reconstruction approach, we also reconstructed the DSI data in MNI-152 space (a standard space introduced by the International Consortium for Brain Mapping, <http://www.bic.mni.mcgill.ca/ServicesAtlases/ICBM152Nlin2009>) using q-space diffeomorphic reconstruction (QSDR) [15], which provides a direct approach to analyze the group difference and also facilitates the comparison using fiber tracking. QSDR is the generalization of GQI that allows users to construct ODFs in any given template space (e.g. MNI space). DSI Studio first calculates the quantitative anisotropy (QA) mapping and then normalizes it to the NTU-90 QAmmap. The NTU-90 atlas is the average of the normalized subject data in the MNI-152 space.

For the fiber-tracking datasets, all fiber tracking was performed using the DSI Studio. In most of clinical studies, an ODF-streamlined region of interest (ROI)-based approach are frequently chosen to discern the difference between the patient and control groups [15]. Depending on various kinds of research objectives, there are several ways available to define the ROIs of the subjects. In QSDR reconstruction approach, we used the normalized ROIs from the JHU White Matter tractography atlas provided by DSI studio [67]; In GQI reconstruction approach, we used the selected ROIs from the JHU atlas and warped it to the subject T1-weighted image space by linear registration. Tracts were generated using an ODF-streamline version of the FACT deterministic tractography algorithm [8, 15], and left and right hemispheres were investigated separately. If an ODF had more than one peak orientation, the initial direction was the primary fiber from the resolved orientations. The advantage of “primary” is the stableness and consistency of the results. Trilinear interpolation was used to estimate the propagation direction. Fiber progression continued with a certain step size like 1 mm (half the spacing for QSDR reconstruction approach), minimum fiber length like 40 mm, and turning angle threshold (usually set at 40°–70°). To smooth each track, the next moving directional estimate of each voxel was weighted by a combination of the previous incoming direction and the nearest fiber orientation. Once tracked, all

streamlines were saved in the TrackVis file format. Segmentation of the fiber tracts was performed with TrackVis software (<http://trackvis.org>).

---

## 2.6 Diffusion MRI Applications in Psychiatric Disorders

Diffusion MRI has been becoming an indispensable tool to investigate a variety of psychiatric disorders such as schizophrenia, major depressive disorder, eating disorders, attention deficit disorder and addictions and so on. It has shed insightful light on our understanding of neural connectivity and how abnormalities in connectivity may contribute to the pathogenesis of psychiatric illnesses. This section will concisely summarize recent applications on those psychiatric diseases with DTI/DSI techniques, specifically restricting our attention to the reward-circuitry based brain disorders.

**Obsessive-Compulsive Disorder (OCD):** Alterations in the WM tracts within the classic cortico-striato-thalamo-cortical (CSTC) circuitry, which has long been implicated in the pathogenesis of OCD [39], were always observed in the literature with DTI method. There have been reported that alterations of FA were observed in many brain regions of OCD patients, such as the anterior cingulate [12, 60], internal capsule [12, 73], white matter in the area superolateral to the right caudate [73], corpus callosum [57, 73], and the right inferior parietal and medial frontal regions [36], the bilateral semiovalcenter extending to the subinsular white matter [45]. However, the conclusions drawn from these current studies have been inconsistent. For example, findings in the FA of the anterior cingulate were particularly mysterious, showing higher values [12], lower values [60], or no changes [36, 45, 73] in OCD patients in comparison to normal subjects.

Findings concerning the anterior thalamic radiations (ATR) seem to be inconsistent as well. Cannistraro et al. [12] reported an increased FA value in the left anterior limb of the internal capsule, whereas Yoo et al. [73] found increases

in FA in the superolateral area of the right caudate that were penetrated by the ATR. These divergent observations by the DTI could be caused by the notoriously complicated structure of the brain network, in which the presence of crossing fibers has been robustly demonstrated by the DSI-based tractography in both nonhuman primate and human [21, 58, 69]. Therefore, Chiu and his co-workers applied the GFA value to describe the microstructural integrity of the white matter tracts [15]. They found significantly lower mean GFA in the right ATR and the left the anterior segment of cingulum bundles in OCD subjects compared to the ATRs and cingulum bundles of normal controls. In addition to the GFA measure, asymmetry of the mean GFA between the left and right tracts was also calculated [15], which might provide a parsimonious explanation to the above discrepancy observed in different reports. Notwithstanding the new evidence, it requires further research to fully elucidate those apparent contradictory results. Besides that, more widespread WM abnormalities like the microstructural alterations in the fronto-basal pathways targeting the orbitofrontal cortex and the anterior cingulate cortex have been proposed to be involved in OCD [39]. Menzies and colleagues reported that the anatomical connectivity between lateral frontal and parietal regions was altered as well as microstructural abnormalities in intra-hemispheric bundles linking distinctive areas of the prefrontal cortex to posterior parietal and occipital association cortices [36].

**Major depressive disorder (MDD):** Decrease in FA was found in the right middle frontal gyrus, left occipitotemporal gyrus, and the subgyral and angular gyri of the right parietal lobe in medication-free young adults with MDD [2]. Lower FA in regions lateral to the anterior cingulate was associated with lower occurring rates of remission in geriatric depression [4]. Older patients with MDD have been shown to demonstrate lower FA in the dorsolateral prefrontal cortex and anterior cingulate cortex [6], and diffuse frontal [2, 47, 63] and temporal lobe [47]. Interestingly, after electroconvulsive therapy (ECT), depressed geriatric patients had an increase in frontal FA associated with the

improvement of their clinical symptoms [46], but not in the temporal WM regions. Diminished FA in white matter regions including anterior cingulate and dorsolateral frontal pathways in patients with late life depression was found to be a strong predictor of poor response to the antidepressant Citalopram [4]. In the future growing psychiatric research with diffusion MRI that points to predicting the disease risks and response factors (ultimately for early intervention or prevention) can be much of translational utility [2].

**Eating Disorder (ED):** Eating disorder is a severe psychiatric disorder associated with self-driven food refusal and emaciation, altered body perception and preoccupations with weight, which generally includes three major categories: Anorexia Nervosa (AN), Bulimia Nervosa (BN) and Eating Disorder Not Otherwise Specified (EDNOS) [29]. In AN patients, Kim and Whalen found that left ventral amygdala responses to fearful versus neutral faces were positively correlated with local FA values along the white matter fibers located within the amygdala-ventromedial prefrontal cortex pathway. Intriguingly, these significantly correlated voxel clusters extended into the left ventral striatum and terminated at the left medial orbitofrontal cortex [30]. The abnormal WM integrity of the limbic and association pathways in AN patients has been found to account for disturbed feeding, emotion processing and body perception. Moreover, changes of FA in the left and right fimbria-fornix were allowed to predict the harm avoidance behavior of AN patients, which suggested that the fimbria-fornix WM pathway is possibly involved in high anxiety level of AN [28]. Frieling and his coworkers identified disturbances of associational and commissural fibers in the bilateral occipitotemporal white matter, suggesting that the distortion of self-body image could be related to microstructural alterations of white matter tracts connecting the extrastriate visual cortex with other brain regions involved in body perception [18]. Moreover, they identified in AN patients bilateral reductions of FA maps in the posterior thalamic radiation including the optic radiation and the left mediodorsal thalamus [18]. On the other hand,

widespread decrease in FA values of BN patients were observed in the bilateral corona radiata extending into the posterior limb of the internal capsule, the corpus callosum, the right subinsular WM, and right fornix. The result suggested that the integrity of WM fiber tracts was largely altered in BN, especially in the corona radiata which was deemed to account for taste and brain reward processing [38].

**Substance Dependence (SD):** Compared with normal controls, both men and women with chronic alcoholism show a decrease in FA in the genu of the CC and the centrum semiovale [48–52]. FA decreases in the splenium of the CC was also found in male subjects [48, 51]. The decrease in FA in the genu was associated with decreased volume of both the genu and the body of the CC, and decreases in FA have been shown to correlate with the amount of alcohol consumption and with comorbid human immunodeficiency syndrome infection [50]. Men with alcohol dependence showed lower generalized FA values on all segments of the corpus callosum. The segment interconnecting the bilateral orbitofrontal cortices was the most affected [15].

Another major SD in our daily life is cocaine use, which can result in a number of neurological complications including headaches, seizures, and strokes. There is evidence that cocaine adversely disrupted the myelin sheaths [41]. DTI studies of cocaine abuse patients reveal a decrease in frontal FA and the genu and rostral body of the CC, and the FA measures in the CC were inversely correlated with impulsivity [35, 36, 40, 70].

## 2.7 Conclusion

The high sensitivity of diffusion MRI technique enables its rising popularity in the diagnosis of psychiatric illnesses and the monitoring of the brain response to therapeutic interventions. One attractive perspective is to follow subjects longitudinally to determine how the microstructural properties of the tissue change over time if each subject serves as their own baseline reference. In

this way, the abnormality at different stage can be well characterized and the therapeutic effects are readily predicted. Diffusion image-based prognostic indicators of disease course and response to therapy would be extremely valuable to assess the responsiveness of patients to specific therapies, since predictive imaging measures would enable earlier interventions. Up to date, there are only a handful of DSI studies to examine the brain architecture and connectivity in psychiatric disorders. Due to differences in methodologies, scanner sequences, and image processing algorithms, it requires more cautions to interpret the physiological meaning of results obtained by the diffusion MRI methods in clinical psychiatric research.

**Acknowledgments** This work was partially supported by The Hundred Talent Program (Technology), Chinese Academy of Sciences (ZW). We thank Franz Schmitt, Renate Jerecic, Thomas Benner, Kecheng Liu, Ignacio Vallines, and Hui Liu for their help and contribution to the construction of our custom-tuned gradient-insert MRI facility.

## References

1. Alexander AL. Analysis of partial volume effects in diffusion-tensor MRI. *Magn Reson Med*. 2001;45: 770–80.
2. Alexander AL, Lee JE, Lazar M, Field AS. Diffusion tensor imaging of the brain. *Neurotherapeutics*. 2007;4:316–29.
3. Alexander DC, Barker GJ. Optimal imaging parameters for fiber-orientation estimation in diffusion MRI. *Neuroimage*. 2005;27:357–67.
4. Alexopoulos GS, Kiosses DN, Choi SJ, Murphy CF, Lim KO. Frontal white matter microstructure and treatment response of late-life depression: a preliminary study. *Am J Psychiatry*. 2002;159: 1929–32.
5. Ardekani BA, Nierenberg J, Hoptman MJ, Javitt DC, Lim KO. MRI study of white matter diffusion anisotropy in schizophrenia. *Neuroreport*. 2003; 14:2025–9.
6. Bae JN, MacFall JR, Krishnan KR, Payne ME, Steffens DC, Taylor WD. Dorsolateral prefrontal cortex and anterior cingulate cortex white matter alterations in late-life depression. *Biol Psychiatry*. 2006;60:1356–63.
7. Bassar PJ, Mattiello J, LeBihan D. MR diffusion tensor spectroscopy and imaging. *Biophys J*. 1994;66:259–67.

8. Basser PJ, Pajevic S, Pierpaoli C, Duda J, Aldroubi A. In vivo fiber tractography using DT-MRI data. *Magn Reson Med*. 2000;44:625–32.
9. Beaulieu C. The basis of anisotropic water diffusion in the nervous system—a technical review. *NMR Biomed*. 2002;15:435–55.
10. Callaghan PT. Principles of Nuclear Magnetic Resonance Microscopy. Oxford: Oxford University Press; 1993.
11. Callaghan PT, Eccles CD, Xia Y. NMR microscopy of dynamic displacements—K-Space and Q-Space Imaging. *J Phys E: Sci Instrum*. 1988;21:820–2.
12. Cannistraro PA, Makris N, Howard JD, Wedig MM, Hodge SM, et al. A diffusion tensor imaging study of white matter in obsessive-compulsive disorder. *Depress Anxiety*. 2007;24:440–6.
13. Catani M. Diffusion tensor magnetic resonance imaging tractography in cognitive disorders. *Curr Opin Neurol*. 2006;19:599–606.
14. Chenevert TL, Brunberg JA, Pipe JG. Anisotropic diffusion in human white matter: demonstration with MR techniques in vivo. *Radiology*. 1990;171:401–5.
15. Chiu CH, Lo YC, Tang HS, Liu IC, Chiang WY, et al. White matter abnormalities of fronto-striato-thalamic circuitry in obsessive-compulsive disorder: a study using diffusion spectrum imaging tractography. *Psychiatry Res*. 2011;192:176–82.
16. Cory DG, Garroway AN. Measurement of translational displacement probabilities by NMR—an indicator of compartmentation. *Magn Reson Med*. 1990;14:435–44.
17. Descoteaux M, Angelino E, Fitzgibbons S, Deriche R. Regularized, fast, and robust analytical Q-ball imaging. *Magn Reson Med*. 2007;58:497–510.
18. Frieling H, Fischer J, Wilhelm J, Engelhorn T, Bleich S, et al. Microstructural abnormalities of the posterior thalamic radiation and the mediodorsal thalamic nuclei in females with anorexia nervosa—a voxel based diffusion tensor imaging (DTI) study. *J Psychiatr Res*. 2012;46:1237–42.
19. Gorczewski K, Mang S, Klose U. Reproducibility and consistency of evaluation techniques for HARDI data. *MAGMA*. 2009;22:63–70.
20. Granziera C, Schmahmann JD, Hadjikhani N, Meyer H, Meuli R, et al. Diffusion spectrum imaging shows the structural basis of functional cerebellar circuits in the human cerebellum in vivo. *PLoS One*. 2009;4:e5101.
21. Hagmann P, Cammoun L, Gigandet X, Meuli R, Honey CJ, Wedeen VJ. Mapping the structural core of human cerebral cortex. *PLoS Biol*. 2008.
22. Hagmann P, Jonasson L, Deffieux T, Meuli R, Thiran JP, Wedeen VJ. Fibertract segmentation in position orientation space from high angular resolution diffusion MRI. *Neuroimage*. 2006;32:665–75.
23. Hagmann P, Thiran JP, Jonasson L, Vanderghenst P, Clarke S, et al. DTI mapping of human brain connectivity: statistical fibre tracking and virtual dissection. *Neuroimage*. 2003;19:545–54.
24. Hsu YC, Hsu CH, Tseng WYI. Correction for susceptibility-induced distortion in echo-planar imaging using field maps and model-based point spread function. *IEEE Trans Med Imaging*. 2009;28:1850–7.
25. Johansen-Berg H. Behavioural relevance of variation in white matter microstructure. *Curr Opin Neurol*. 2010;23:351–8.
26. Johansen-Berg H, Behrens TEJ. Diffusion MRI: from quantitative measurement to in-vivo neuroanatomy. In: Johansen-Berg H, Behrens TEJ, editors. *Diffusion MRI*. San Diego: Academic Press; 2009.
27. Jones DK, Knosche TR, Turner R. White matter integrity, fiber count, and other fallacies: the do's and don'ts of diffusion MRI. *Neuroimage*. 2013;73:239–54.
28. Kazlouski D, Rollin MD, Tregellas J, Shott ME, Jappe LM, et al. Altered fimbria-fornix white matter integrity in anorexia nervosa predicts harm avoidance. *Psychiatry Res*. 2011;192:109–16.
29. Keel PK, Brown TA, Holland LA, Bodell LP. Empirical classification of eating disorders. *Annu Rev Clin Psychol*. 2012;8:381–404.
30. Kim MJ, Whalen PJ. The structural integrity of an amygdala-prefrontal pathway predicts trait anxiety. *J Neurosci*. 2009;29:11614–8.
31. Kuo LW, Chen JH, Wedeen VJ, Tseng WY. Optimization of diffusion spectrum imaging and q-ball imaging on clinical MRI system. *Neuroimage*. 2008;41:7–18.
32. Kyriakopoulos M, Frangou S. Recent diffusion tensor imaging findings in early stages of schizophrenia. *Curr Opin Psychiatry*. 2009;22:168–76.
33. Le Bihan D. Looking into the functional architecture of the brain with diffusion MRI. *Nat Rev Neurosci*. 2003;4:469–80.
34. Le Bihan D, Breton E, Lallemand D, Grenier P, Cabanis E, Laval-Jeantet M. MR imaging of intravoxel incoherent motions: application to diffusion and perfusion in neurologic disorders. *Radiology*. 1986;161:401–7.
35. Lim KO, Wozniak JR, Mueller BA, Franc DT, Specker SM, et al. Brain macrostructural and microstructural abnormalities in cocaine dependence. *Drug Alcohol Depend*. 2008;92:164–72.
36. Menzies L, Chamberlain SR, Laird AR, Thelen SM, Sahakian BJ, Bullmore ET. Integrating evidence from neuroimaging and neuropsychological studies of obsessive-compulsive disorder: the orbitofronto-striatal model revisited. *Neurosci Biobehav Rev*. 2008;32:525–49.
37. Merboldt K-D, Hanicke W, Frahm J. Self-diffusion NMR imaging using stimulated echoes. *J Magn Reson*. 1985;64:479–86.
38. Mettler LN, Shott ME, Pryor T, Yang TT, Frank GK. White matter integrity is reduced in bulimia nervosa. *Int J Eat Disord*. 2013;46:264–73.
39. Milad MR, Rauch SL. Obsessive-compulsive disorder: beyond segregated cortico-striatal pathways. *Trends Cogn Sci*. 2012;16:43–51.

40. Moeller FG, Hasan KM, Steinberg JL, Kramer LA, Dougherty DM, et al. Reduced anterior corpus callosum white matter integrity is related to increased impulsivity and reduced discriminability in cocaine-dependent subjects: diffusion tensor imaging. *Neuropsychopharmacology*. 2005;30:610–7.
41. Moeller FG, Hasan KM, Steinberg JL, Kramer LA, Valdes I, et al. Diffusion tensor imaging eigenvalues: preliminary evidence for altered myelin in cocaine dependence. *Psychiatry Res*. 2007;154:253–8.
42. Mori S, van Zijl PCM. Fiber tracking: principles and strategies—a technical review. *NMR Biomed*. 2002;15:468–80.
43. Mori S, Zhang J. Principles of diffusion tensor imaging and its applications to basic neuroscience research. *Neuron*. 2006;51:527–39.
44. Moseley ME, Cohen Y. Diffusion-weighted MR imaging of anisotropic water diffusion in cat central nervous system. *Radiology*. 1990;176:439–45.
45. Nakamae T, Narumoto J, Shibata K, Matsumoto R, Kitabayashi Y, et al. Alteration of fractional anisotropy and apparent diffusion coefficient in obsessive-compulsive disorder: a diffusion tensor imaging study. *Prog Neuropsychopharmacol Biol Psychiatry*. 2008;32:1221–6.
46. Nobuhara K, Okugawa G, Minami T, Takase K, Yoshida T, et al. Effects of electroconvulsive therapy on frontal white matter in late-life depression: a diffusion tensor imaging study. *Neuropsychobiology*. 2004;50:48–53.
47. Nobuhara K, Okugawa G, Sugimoto T, Minami T, Tamagaki C, et al. Frontal white matter anisotropy and symptom severity of late-life depression: a magnetic resonance diffusion tensor imaging study. *J Neurol Neurosurg Psychiatry*. 2006;77:120–2.
48. Pfefferbaum A, Adalsteinsson E, Sullivan EV. Dismorphology and microstructural degradation of the corpus callosum: interaction of age and alcoholism. *Neurobiol Aging*. 2006;27:994–1009.
49. Pfefferbaum A, Adalsteinsson E, Sullivan EV. Supratentorial profile of white matter microstructural integrity in recovering alcoholic men and women. *Biol Psychiatry*. 2006;59:364–72.
50. Pfefferbaum A, Rosenbloom MJ, Adalsteinsson E, Sullivan EV. Diffusion tensor imaging with quantitative fibre tracking in HIV infection and alcoholism comorbidity: synergistic white matter damage. *Brain*. 2007;130:48–64.
51. Pfefferbaum A, Sullivan EV. Microstructural but not macrostructural disruption of white matter in women with chronic alcoholism. *Neuroimage*. 2002;15:708–18.
52. Pfefferbaum A, Sullivan EV. Disruption of brain white matter microstructure by excessive intracellular and extracellular fluid in alcoholism: evidence from diffusion tensor imaging. *Neuropsychopharmacology*. 2005;30:423–32.
53. Pierpaoli C. Diffusion tensor MR imaging of the human brain. *Radiology*. 1996;201:637–48.
54. Pierpaoli C, Basser PJ. Toward a quantitative assessment of diffusion anisotropy. *Magn Reson Med*. 1996;36:893–906.
55. Reese TG, Heid O, Weisskoff RM, Wedeen VJ. Reduction of eddy-current-induced distortion in diffusion MRI using a twice-refocused spin echo. *Magn Reson Med*. 2003;49:177–82.
56. Roberts RE, Anderson EJ, Husain M. White matter microstructure and cognitive function. *Neuroscientist*. 2013;19:8–15.
57. Saito Y, Nobuhara K, Okugawa G, Takase K, Sugimoto T, et al. Corpus callosum in patients with obsessive-compulsive disorder: diffusion-tensor imaging study. *Radiology*. 2008;246:536–42.
58. Schmahmann JD, Pandya DN, Wang R, Dai G, D’Arceuil HE, et al. Association fibre pathways of the brain: parallel observations from diffusion spectrum imaging and autoradiography. *Brain*. 2007;130:630–53.
59. Stejskal EO, Tanner JE. Spin diffusion measurements: spin echoes in the presence of a time-dependent field gradient. *J Chem Phys*. 1965;42:288–292.
60. Szeszko PR, MacMillan S, McMeniman M, Lorch E, Madden R, et al. Amygdala volume reductions in pediatric patients with obsessive-compulsive disorder treated with paroxetine: preliminary findings. *Neuropsychopharmacology*. 2004;29:826–32.
61. Tang PF, Ko YH, Luo ZA, Yeh FC, Chen SH, Tseng WY. Tract-specific and region of interest analysis of corticospinal tract integrity in subcortical ischemic stroke: reliability and correlation with motor function of affected lower extremity. *Am J Neuroradiol*. 2010;31:1023–30.
62. Taylor DG, Bushell MC. The spatial-mapping of translational diffusion-coefficients by the NMR imaging technique. *Phys Med Biol*. 1985;30:345–9.
63. Taylor WD, MacFall JR, Payne ME, McQuoid DR, Provenzale JM, et al. Late-life depression and microstructural abnormalities in dorsolateral prefrontal cortex white matter. *Am J Psychiatry*. 2004;161:1293–6.
64. Tuch DS. Q-ball imaging. *Magn Reson Med*. 2004;52:1358–72.
65. Tuch DS, Reese TG, Wiegell MR, Makris N, Belliveau JW, Wedeen VJ. High angular resolution diffusion imaging reveals intravoxel white matter fiber heterogeneity. *Magn Reson Med*. 2002;48:577–82.
66. Tuch DS, Reese TG, Wiegell MR, Wedeen VJ. Diffusion MRI of complex neural architecture. *Neuron*. 2003;40:885–95.
67. Wakana S, Caprihan A, Panzenboeck MM, Fallon JH, Perry M, et al. Reproducibility of quantitative tractography methods applied to cerebral white matter. *Neuroimage*. 2007;36:630–44.
68. Wedeen VJ, Hagmann P, Tseng WY, Reese TG, Weisskoff RM. Mapping complex tissue architecture with diffusion spectrum magnetic resonance imaging. *Magn Reson Med*. 2005;54:1377–86.



- 
69. Wedeen VJ, Rosene DL, Wang R, Dai G, Mortazavi F, et al. The geometric structure of the brain fiber pathways. *Science*. 2012;335:1628–34.
  70. Wedeen VJ, Wang RP, Schmahmann JD, Benner T, Tseng WY, et al. Diffusion spectrum magnetic resonance imaging (DSI) tractography of crossing fibers. *Neuroimage*. 2008;41:1267–77.
  71. Wiegell MR. Fiber crossing in human brain depicted with diffusion tensor MR imaging. *Radiology*. 2000;217.
  72. Yeh FC, Wedeen VJ, Tseng WY. Generalized q-sampling imaging. *IEEE Trans Med Imaging*. 2010;29:1626–35.
  73. Yoo SY, Jang JH, Shin YW, Kim DJ, Park HJ, et al. White matter abnormalities in drug-naïve patients with obsessive-compulsive disorder: a diffusion tensor study before and after citalopram treatment. *Acta Psychiatr Scand*. 2007;116:211–9.

Neurosurgical Treatments for Psychiatric Disorders

Sun, B.; Salles, A.D. (Eds.)

2015, XIV, 228 p. 59 illus., 38 illus. in color., Hardcover

ISBN: 978-94-017-9575-3